

## HIGHLY LOADED SILVER AND COPPER(II) OXIDE NANOPARTICLE INKS FOR ADDITIVE MANUFACTURING OF ELECTRONICS

**E. Dimitriou<sup>1,2</sup>, N. Michailidis<sup>1,2,\*</sup>**

<sup>1</sup>Physical Metallurgy Laboratory, Mechanical Engineering Department, School of Engineering,  
Aristotle University of Thessaloniki, 54124, Thessaloniki, Greece

<sup>2</sup>Centre for Research & Development of Advanced Materials (CERDAM),  
Center for Interdisciplinary Research and Innovation, Balkan Centre, Building B',  
10<sup>th</sup> km Thessaloniki-Thermi Road, 57001, Thessaloniki, Greece

(\*[nmichail@auth.gr](mailto:nmichail@auth.gr))

### ABSTRACT

In recent years, significant progress has been made in the additive microfabrication of electronic components. Colloidal nanoparticle-based conductive inks represent the most popular functional material for printing of electronics. Laser-induced forward transfer (LIFT) follows the demand for miniaturized electronic components, by increasing the printing speed and resolution. This study focuses on the preparation of highly loaded silver and copper(II) oxide nanoparticle – based inks for LIFT applications. Suspensions of 25% w/w solids loading in glycol – water co-solvent media have been successfully prepared and characterized. The nanoinks exhibited exceptional colloidal stability in the course of one month, high viscosity (> 5 Pa·s), non-Newtonian, shear-thinning behaviour and particles smaller than 35 nm, thus properties compatible to the LIFT technique. The low evaporation rate of the suspension media and the sintering behavior of the particles under heating further showcased their potential for LIFT applications.

**KEYWORDS:** Additive Manufacturing, Conductive Inks, Nanotechnology, Silver Nanoparticles, Copper Oxide Nanoparticles

### INTRODUCTION

Recent years have witnessed significant progress in the additive microfabrication of electronic components, transitioning from experimental proofs-of-concept in laboratories to industrial manufacturing processes. As the demand for miniaturized electronics grows, there is a corresponding need for advanced patterning techniques and innovative nanotechnology-based materials <sup>[1,2]</sup>. Laser-induced forward transfer (LIFT) addresses this demand by enhancing printing speed (> 1 m/s) and resolution (< 50 μm) while minimizing the heat affected zone <sup>[2]</sup>. LIFT utilizes a pulsed laser beam to project material from a thin film donor onto a receiver substrate based on digitally defined presets (Figure 1) <sup>[3]</sup>. Subsequent to printing, sintering with laser or conventional heating is typically employed, to obtain conductive components <sup>[2]</sup>.

Functional nanotechnology-based conductive inks represent the most promising materials in the fabrication of micron-sized conductive patterns <sup>[4]</sup>. Typically, these inks comprise suspensions of metallic nanoparticles stabilized by surfactants and ligand shells, dispersed in either aqueous or organic media. These ligands, known as capping agents, serve to prevent particle agglomeration. During sintering of the printed parts, these capping agents can be removed, facilitating physical contact between the particles and thus the formation of a conductive path.

Until today, most attention has focused on silver and gold nanoparticle inks due to their chemical stability and electrical conductivity. Efforts are underway to enhance the chemical stability of copper nanoinks, a potential alternative to expensive noble metal inks, by controlling oxidation through atmospheric conditions or utilizing copper oxide nanoparticles in printable inks <sup>[5]</sup>.

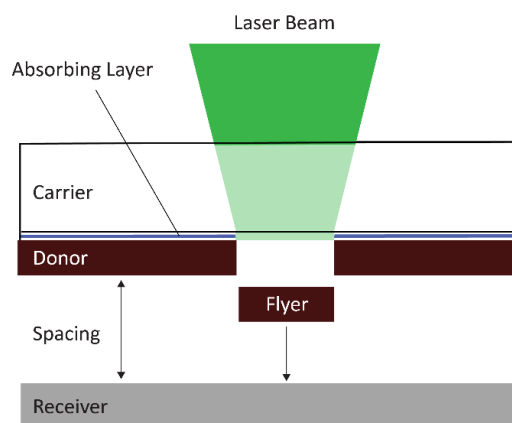


**Figure 1.** The principle of LIFT.

LIFT, being a non-contact and nozzle-free printing method, offers tolerance for anisotropic nanostructures and larger particle sizes [3]. However, spherical particles facilitate long-term colloidal stability, rheological control and sintering at lower temperatures [1]. LIFT favors high viscosity (up to  $10^3$  Pa·s), non-Newtonian, shear-thinning inks, which respond to the significant shear stress induced by laser pulses, ensuring smooth material deposition and fine printed patterns [2]. Additionally, the tolerance of LIFT for viscous inks enables printing of highly loaded inks, which is advantageous for achieving high conductivity [3]. Finally, LIFT prefers non-volatile ink media, enabling smooth solvent evaporation [2,6].

Despite the attention received by LIFT, there has been relatively little emphasis on the inks used with this technique [6]. Many researchers employing LIFT rely on commercial inks designed for traditional printing techniques like screen printing [7]. This study concentrates on developing high-content silver (AgNPs) and copper(II) oxide nanoparticle (CuONPs) inks with properties (nanoparticle size and shape, ink rheology, chemical stability and thermal properties) tailored to match the processing parameters of LIFT.

## METHODOLOGY

The nanoparticles used in this study were synthesized by PLiN Nanotechnology SA. The particles were available in the form of aqueous suspensions, their average diameter was approximately 4 nm with narrow distribution, and their concentration was 1500 ppm. Additionally, they were spherical and covered by an animal protein, acting as a stabilizing agent [8,9]. The pH of their suspensions was around 4 and 10, respectively. Sodium hydroxide (NaOH) of  $\geq 98\%$  purity and deionized water were used for the preparation of an aqueous 6M NaOH solution. Hydrochloric acid (HCl) solution, 37% a.r., acetone of  $\geq 99\%$  purity and ethylene glycol, 1,3-propylene glycol, 1,2-propylene glycol and glycerol were used as received. The glycols were selected as the main solvent of the inks prepared due to their high viscosity and boiling point.

For the preparation of highly loaded AgNPs suspensions, 4L of acetone were added to 1L of the initial AgNPs suspension. The beaker was sealed with membrane and the suspension was stored at rest for the particles to participate overnight. The main volume of the supernatant was discarded and the particles were separated from the rest of the volume via centrifugation under 10,000 xg for 5 min. The sediment was dried overnight under atmosphere. Next, it was pulverized with a mortar. Suspensions of 25% w/w solids loading were prepared by redispersion of weighed particle quantities into a mixture of deionized water and the respective glycol in a 4:6 mass ratio under overnight mechanical stirring. The glycols most compatible with the AgNPs were ethylene glycol, 1,2-propylene glycol and glycerol.

The procedure for the preparation of high-content CuONPs has been described elsewhere [10]. Suspensions of 25% w/w solids loading were prepared in a mixture of NaOH solution and the respective glycol in a 1:10 mass ratio. The presence of NaOH served the purpose of restoring the pH

of the final suspensions to alkaline values. The glycols most compatible with the CuONPs were ethylene glycol, 1,3-propylene glycol and 1,2-propylene glycol.

The sample media will be referred to as EG/W (ethylene glycol and water), 1,3PrG/W (1,3-propylene glycol and water), 1,2PrG/W (1,2-propylene glycol and water) and G/W (glycol and water), respectively.

The optical properties of the suspensions were analyzed via UV-visible Spectroscopy. Absorbance spectra were collected for each sample, on the day of preparation and after 1 month, using a double beam Shimadzu UV-1800 spectrophotometer and quartz cuvettes with a path length of 10 mm. The spectral bandwidth ranged from 200 to 800 nm at a wavelength resolution of 2 nm. The instrument was controlled using the UV Probe software package. The samples were prepared by dilution of 1 g of each suspension with 400 g and 70 g of the corresponding medium in the case of AgNPs and CuONPs, respectively. Additionally, in the case of the dilute CuONPs samples, the pH was regulated to 10. The medium of each sample was used as blank.

Nanoscale investigation was carried out with a high resolution JEOL JEM-2100 LaB<sub>6</sub> transmission electron microscope (HRTEM), operating at 200 kV. The samples under investigation (~0.2 ml) were suspended in deionized water and treated with ultrasound to disaggregate the agglomerated particles. A drop from the suspension was then placed on a 300-mesh carbon coated copper grid and air-dried overnight.

Rheological measurements were performed using a rotational TA Instruments Discovery Hybrid Rheometer HR 20, with a parallel plate setup in an Environmental Test Chamber (ETC). The measurement temperature was 25 °C. The measurement parameters were controlled using the TRIOS software package. Viscosity values were collected as a function of shear rate in a 10<sup>-2</sup> – 10<sup>5</sup> μN·m torque range. Steady state sensing was performed with 5 points per decade of torque values, maximum equilibration time of 90 s, sample period of 10 s and 5% tolerance.

Thermogravimetric analysis (TGA) was performed using the TA Instruments Discovery Simultaneous Thermal Analyzer SDT 650. The measurements were carried out on approximately 10 mg of each sample in an alumina pan, under nitrogen atmosphere. The weight percentage was recorded as a function of temperature, in a temperature range of 50-250 °C, with a heating rate of 50 °C/min (weighing accuracy of ±0.5% and precision of ±0.1%). The instrument was controlled using the TRIOS software package.

Next, the sintering behavior of the nanoinks was evaluated. The AgNPs inks were coated onto a glass substrate (glass microscope slides) with an automatic applicator. The film thickness was regulated at 0.1 mm and the coating rate at 50 mm/s. Then, the films were “pre-baked” inside a dryer at 70 °C for different times (depending on the sample, the drying time ranged from 1h to overnight) and sintered inside an oven under argon atmosphere. Two heating regimes were tested: (1) heating with a rate of 10 °C/min to 150, 200, 250, 300, 350 or 400 °C and (2) the same procedure followed by isothermal heating at the end temperature for 1h.

In the case of CuONPs the sintering process was more complex, since it required the reduction of Cu(II) to Cu(0) prior to sintering. The CuONPs were subject to two heating rounds in TGA, one from room temperature to 275 °C, with a heating rate of 50 °C/min, under nitrogen atmosphere, aiming at the evaporation of the solvents, and one from 50 °C to 150, 200, 250, 300, 350 or 400 °C under hydrogen 5% v/v in argon. Between the rounds, the sample was cooled down to 50 °C. Isothermal heating at the end temperature of the second round has also been investigated.

The sintered particles were analyzed with Scanning Electron Microscopy (SEM), using Phenom ProX G6, Thermo Fischer Scientific, with long lifetime thermionic source (CeB6), light optical magnification range: 20–134x and electron optical magnification range: 160–350,000x.

## RESULTS AND DISCUSSION

Figure 2 presents the UV-visible spectra collected. The absorbance data of the AgNPs

samples confirmed the spherical size of the particles, due to the characteristic surface plasmon resonance peak at approximately 425 nm <sup>[4]</sup>. Furthermore, the spectra suggested monomodal and narrow size distribution. CuONPs samples exhibited a single peak around 550 nm, suggesting monomodal size distribution. Small variations were observed in the absorption data of all samples in the course of a month, showcasing their excellent colloidal stability.

The HRTEM images obtained from the AgNPs showed spherical particles of uniform size distribution. Although the concentration process seemed to affect their size, they were smaller than 35 nm in all three AgNPs samples. The HRTEM results of the CuONPs samples showed spherical particles with diameters of a few nanometers overlapping each other and forming flower-like clusters. Similar aggregation behavior has been previously reported in the literature <sup>[11,12]</sup>. However, it can be attributed to the limitations of the HRTEM technique in the preparation of the samples <sup>[12]</sup>. Figure 3 presents indicative HRTEM images of the AgNPs (a) and CuONPs (b) obtained from the respective suspensions in EG/W.

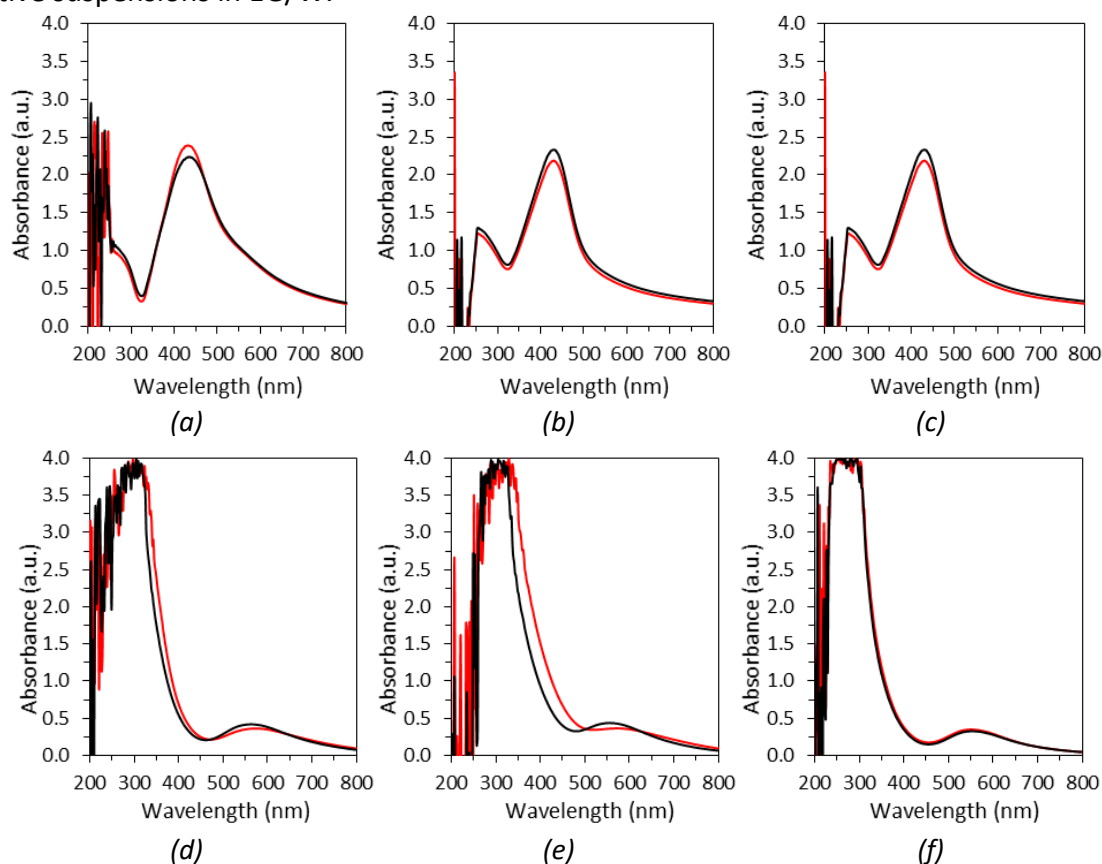


**Figure 2.** UV-Visible absorption spectra of the AgNPs suspension in EG/W (a), 1,2PrG/W (b) and G/W (c), and the CuONPs suspension in EG/W (d), 1,3-PrG/W (e) and 1,2PrG/G (f) on the day of preparation (black) and after 1 month (red).

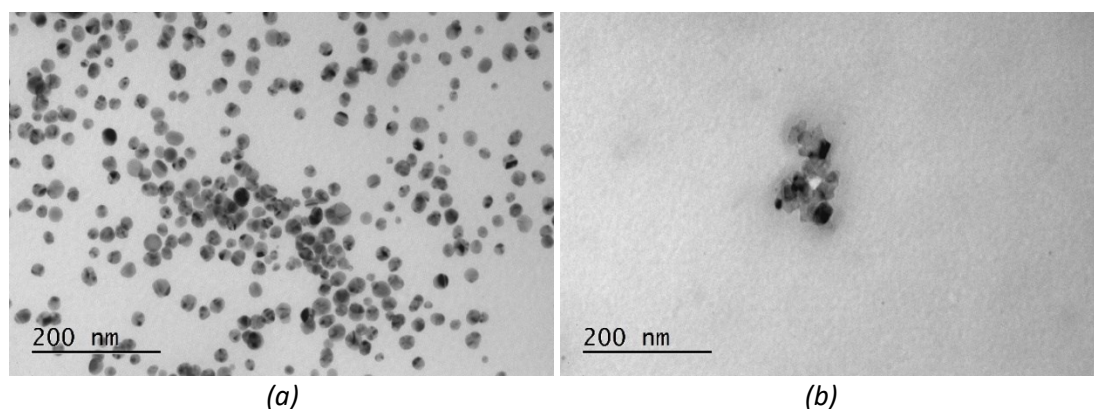


**Figure 3.** HRTEM images of the AgNPs (a) and CuONPs (b) obtained from the respective suspensions in EG/W.

The results of the rheological measurements demonstrated the non-Newtonian, shear thinning behavior of all inks. Figure 4 demonstrates indicative results obtained from the CuONPs suspensions. The zero-shear viscosity was determined using the Williamson model, at  $6.12 \cdot 10^3$ ,  $1.60 \cdot 10^2$  and  $5.25$  Pa·s, respectively.

Figure 5 presents the weight percentage as a function of temperature obtained via TGA from the AgNPs (a) and CuONPs (b) samples and the respective suspension media. Due to the two-stage evaporation, corresponding to the evaporation of the two solvents in each sample, the media were smoothly removed from the sample during heating. The AgNPs samples, having a glycol : deionized water mass ratio of 6:4, exhibited faster solvent evaporation in comparison to the CuONPs samples, having a solvent mass ratio of 10:1. In all cases, evaporation was complete at 275 °C and the weight percentage curve reached a plateau, confirming that the particle content of the samples was 25% w/w.

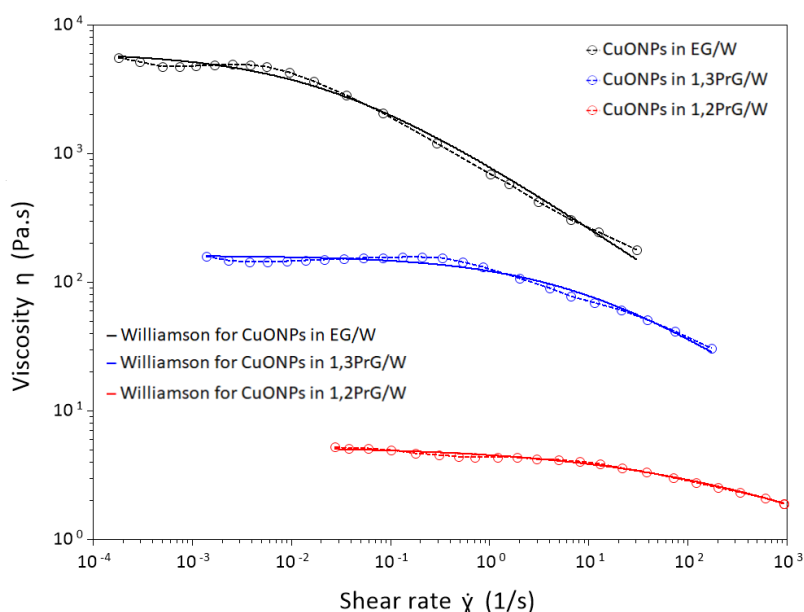


**Figure 4.** Viscosity of the CuONPs suspensions in EG/W (black), 1,3PrG/W (blue) and 1,2PrG/W (red) as a function of shear rate.

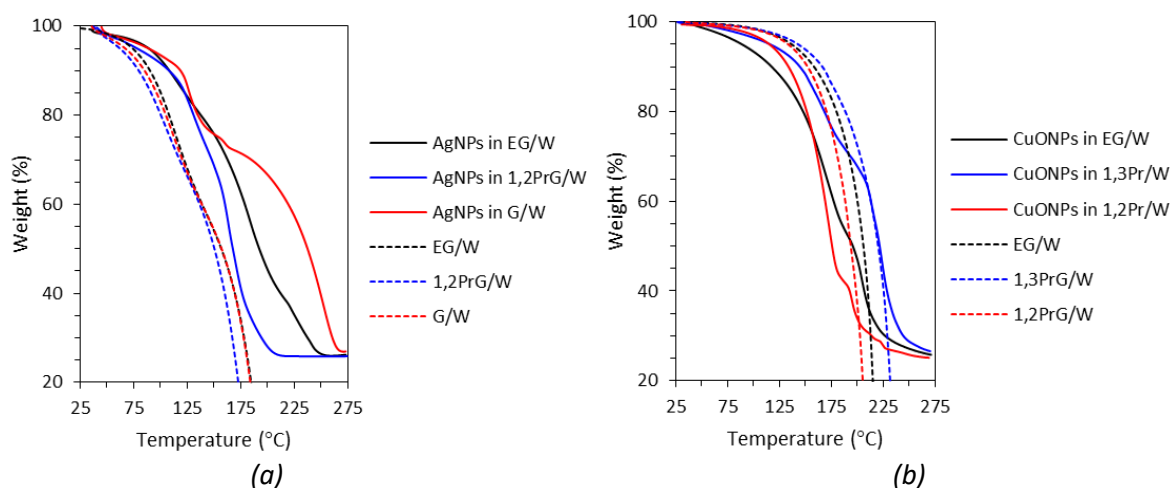


**Figure 5.** Weight (%) as a function of temperature for the AgNPs (a) and the CuONPs (b) suspensions and the respective suspension media.

Figure 6 presents indicative SEM images (magnification 15,500x) obtained from the AgNPs ink in G/W after pre-baking and heating to different end temperatures. Figure 6 (a) shows the formation of “necks” between the particles. In figure 6 (b) necking has advanced and cracks have been formed between the particle clusters due to further drying. In figure 6 (c) the cracks are narrower and in figure 6 (d) surface roughness has reduced significantly.

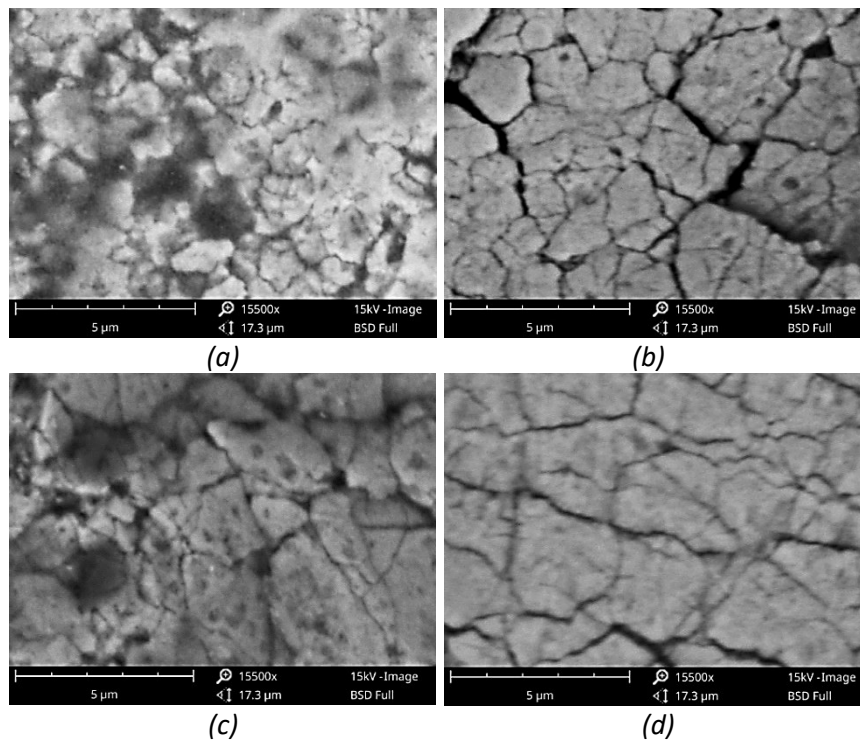


**Figure 6.** AgNPs in G/W after pre-baking and sintering via heating from room temperature to 150 (a), 200 (b), 250 (c) and 300 °C (d).

The results showcased the potential of the inks for LIFT applications. The spherical shape of the nanoparticles contributed to colloidal stability and control of rheology. The small size of the nanoparticles suggested they would require low sintering temperatures, which was confirmed by the sintering tests. The glycol-water co-solvent media not only facilitated good dispersion of the particles but also imparted high viscosity and boiling points to the suspensions, making them compatible to the LIFT processing parameters.

## ACKNOWLEDGEMENTS

This research has been co-financed by the European Union and Greek national funds through the Operational Program Competitiveness, Entrepreneurship and Innovation, under the call RESEARCH – CREATE – INNOVATE (project code: T1EDK-00814). The authors would like to acknowledge the work of the Physical Metallurgy Laboratory of the School of Mining and Metallurgical Engineering of the National Technical University of Athens in carrying out the TEM investigations and PLiN Nanotechnology SA for supplying the nanoparticles used in this study.

## LITERATURE

- [1] Hon, K. K. B., Li, L. & Hutchings, I. M. *CIRP Ann. - Manuf. Technol.* **57**, 601–620 (2008).
- [2] Koritsoglou, O. *et al. Opt. Mater. Express* **9**, 3046 (2019).
- [3] Serra, P. & Piqué, A. *Adv. Mater. Technol.* **4**, 1–33 (2019).
- [4] Rajan, K. *et al. Nanotechnol. Sci. Appl.* **9**, 1–13 (2016).
- [5] Zenou, M. & Grainger, L. Elsevier Inc., 2018.
- [6] Kalaitzis, A. *et al. Appl. Surf. Sci.* **465**, 136–142 (2019).
- [7] Piqué, A., Kim, H., Auyeung, R. C. Y., Beniam, I. & Breckenfeld, E. *Appl. Surf. Sci.* **374**, 42–48 (2016).
- [8] Varympopi, A. *et al. Pathogens* **9**, 1–14 (2020).
- [9] Ntasiou, P. *et al. Nanomaterials* **11**, 1–19 (2021).
- [10] Dimitriou, E. & Michailidis, N. *Eur. J. Mater.* **4**, (2024).
- [11] Jeong, S. W. & Kim, S. D. *J. Environ. Monit.* **11**, 1595–1600 (2009).
- [12] Buazar, F., Sweidi, S., Badri, M. & Kroushawi, F. *Green Process. Synth.* **8**, 691–702 (2019).